

Grafted Biomembranes Containing Membrane Proteins - The Case for the Leucine Transporter

Vivien Jagalski,^{1‡} Robert D. Barker,^{2‡} Mikkel B. Thygesen,¹ Kamil Gotfryd,^{3#} Mie B. Krüger,³ Lei Shi,⁴ Selma Maric,⁵ Nicolas Bovet,¹ Martine Moulin,² Michael Haertlein,² Thomas Günther Pomorski,⁶ Claus J. Loland³ and Marité Cárdenas^{1,5*}

¹Department of Chemistry and Nano-Science Center, University of Copenhagen. Universitetsparken 5, DK 2100, Copenhagen, Denmark and Thorvaldsensvej 40, DK-1871 Frederiksberg C, Denmark.

²Institute Laue Langevin, 71 avenue des Martyrs, CS 20156, 38042 Grenoble Cedex 9, France.

³Department of Neuroscience and Pharmacology, Faculty of Health and Medical Sciences, University of Copenhagen, DK-2200, Copenhagen, Denmark

[#] Present address: Department of Biomedical Sciences Faculty of Health and Medical Sciences, University of Copenhagen, DK-2200, Copenhagen, Denmark

⁴Department of Physiology and Biophysics and Institute for Computational Biomedicine, Weill Cornell Medical College, New York, 10065, USA.

⁵Centre for Membrane Pumps in Cells and Disease (PUMPKIN), Department of Plant and Environmental Sciences, University of Copenhagen, Thorvaldsensvej 40, DK-1871 Frederiksberg C, Denmark.

⁶Malmö University, Biofilm – Research center for Biointerfaces and Department of Biomedical Science, Health & Society, 20506 Malmö, Sweden.

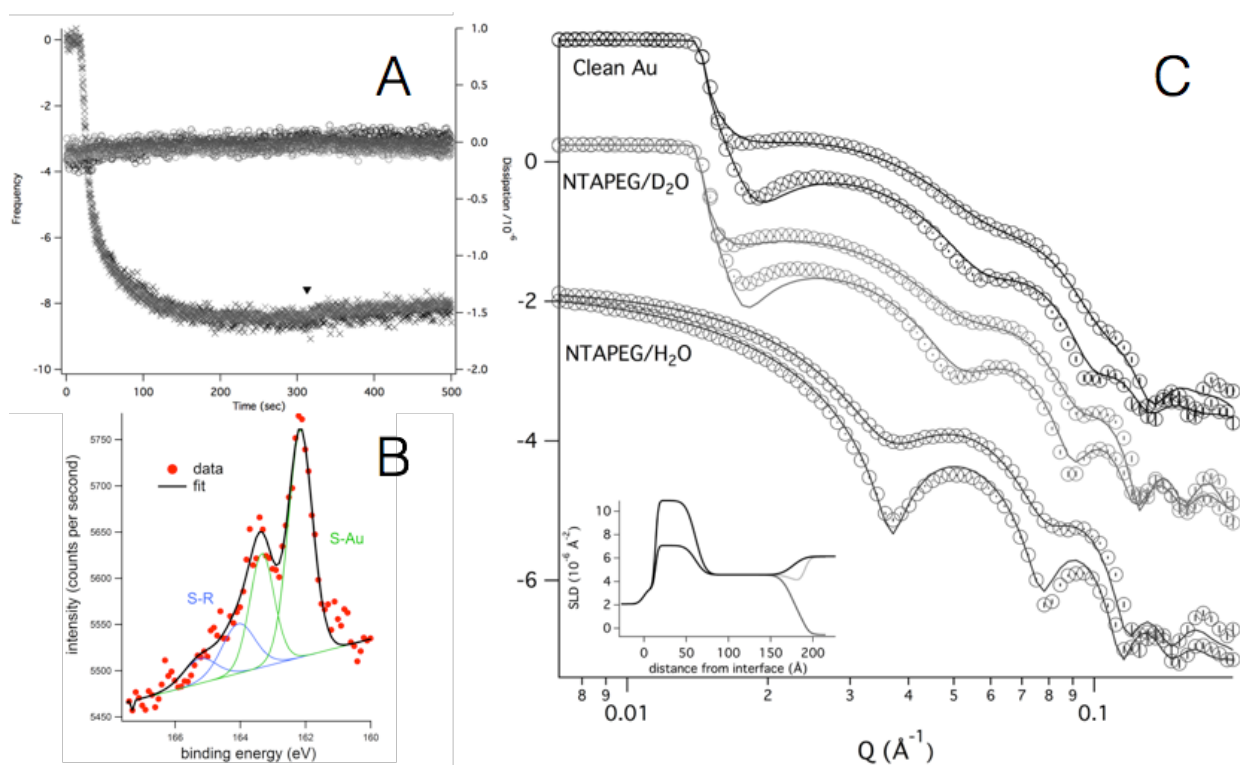


Figure S11. Structural and compositional analysis of the NTA-PEG SAM. (A) NTA-PEG coated Au surfaces were formed by exposure of a 1 mg/mL NTA-PEG solution containing 10 mol% of the linker NTA in ethanol at 14 °C. A self-assembled monolayer (SAM) formed within less than 5 min as determined by quartz crystal microbalance with dissipation (QCM-D) at a flow rate of 100 mL/min. At $t = 0$ sec, the solution was flushed into the cell leading to a significant change in frequency and minimal change in dissipation. These traces are consistent with thin layer highly coupled to the Au sensor. Moreover, the NTA-PEG coating is bound irreversibly since no change in frequency or dissipation occurred upon rinsing with pure ethanol ($t = 310$ sec, marked with an arrow). (B) High resolution XPS spectra for S 2p region for SEM obtained by mixing NTA-PEG (75%) and PEG thiols (25%) in ethanol. The green doublet, S 2p_{3/2} at 162 eV, corresponds to S atoms bound to Au. This shows that the ratio of bound to unbound thiols¹ was very high, suggesting that the coating was formed mainly via the thiol bond, and this process did not depend on the solvent used for deposition (we used pure ethanol, ethanol/water 1:1 in volume, or PBS buffer pH 7.4). However, the coating NTA-PEG/PEG composition depended on the solvent used for coating deposition as estimated from the ratio of N to S-Au peaks and taking into account that each NTA-PEG molecule carries one S per molecule while each PEG molecule carries two S per molecule. This analysis tells us that the estimated actual composition of NTA-PEG was 39, 16 and 66% for depositions in buffer, ethanol-water and ethanol respectively. The fact that the actual composition of the coating

differs from the nominal composition of the solution is not surprising. This will depend on the relative affinities of each type of molecule for the Au surface and the difference in solubility between them. Moreover, XPS can be used to estimate the thickness of the layers and this gives a value of ~ 2.7 nm for NTAPEG and 1 nm for PEG. (C) SAM made by mixtures containing 10% NTA-PEG were characterized with magnetic contrast neutron polarized reflection and the data prior and after coating (symbols). The best fits (full lines) giving a total thickness of 16 Å and a surface coverage of $\sim 50\%$ (inset in C shows the scattering length density profile for the best fit obtained).

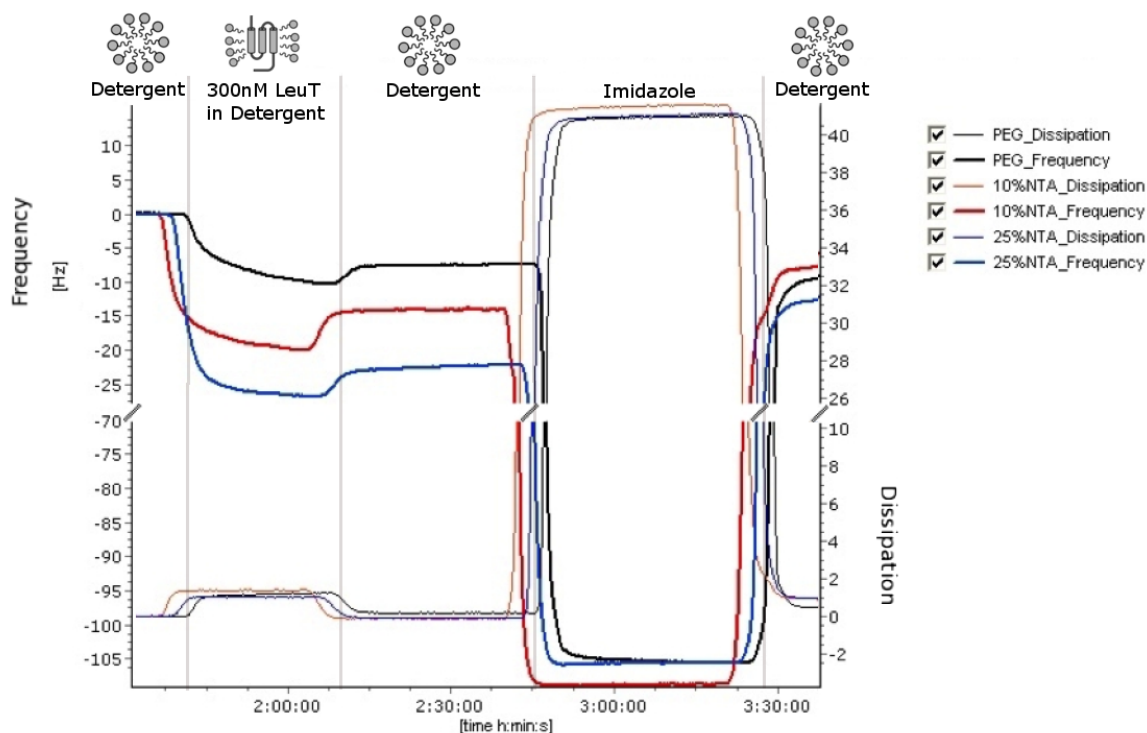


Figure S12. Frequency and dissipation QCM-D traces (7th overtone) as a function of time for the binding of 300 mM LeuT at 20 °C on surfaces functionalized with different NTA-PEG ratios: 0% NTA (black), 10% NTA (red) and 25% NTA (blue). First, the surface was exposed to detergent in order to avoid its dilution upon protein binding. Then, the protein was added to the surface under continuous flow for 10 min. This was immediately followed by rinsing with detergent (DDM) enriched buffer, which removed the protein weakly bound to the surface. After the signal stabilized (no changes above 1 Hz/h), an imidazole wash (500 mM) served to remove his-tag bound protein. A final rinse with detergent rich buffer was performed in order to compare the QCM-D signals at the beginning and at the end of the experiment. The remaining signal after imidazole and detergent wash refers to the protein mass due to non-specific binding e.g. electrostatic and van der Waals interactions. The change in QCM-D signals that can be removed with the imidazole/detergent wash is due to specific bound protein to the Cu²⁺-NTA moiety. The data clearly show that imidazole/buffer washes fail to remove any adsorbed protein on pure PEG surfaces, while NTA containing surfaces show a significant loss of mass. For 10 mol% NTA-PEG coating, the unspecific binding of LeuT is smaller than on pure PEG surfaces. Thus, the QCM-D data suggest that His-tagged LeuT binds to the functionalized surfaces primarily in a specific manner and that the amount of unspecific bound protein can be optimized by varying the NTA-PEG ratio. These data are summarized in Figure S13.

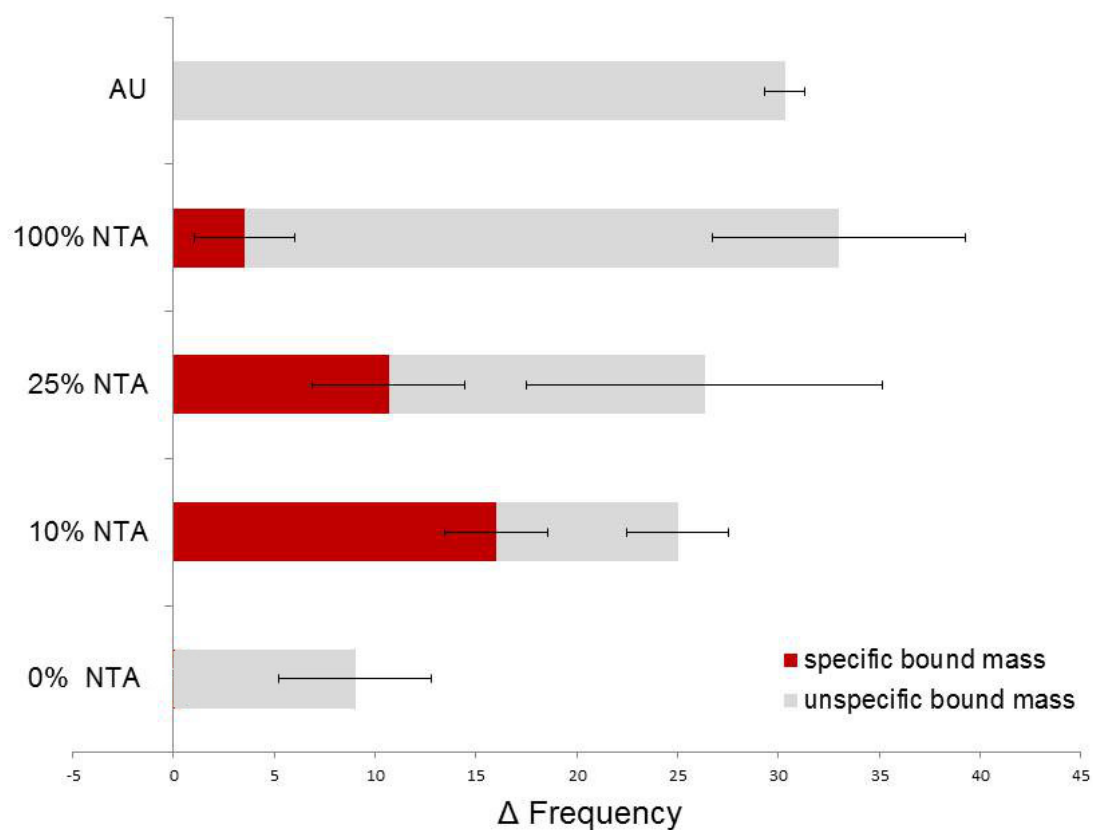


Figure S13. Specific and non-specific protein binding for 300 nM LeuT to various NTA-PEG SAM compositions in terms of the relative change in frequency prior and after treatment with imidazole and surfactant solution at 20 °C. In all cases there was some non-specific binding and the extent of which increases significantly with NTA-PEG linker content. For 10% NTA-PEG - 90% PEG, minimal non-specific LeuT binding occurs as the signal is slightly lower to the SAM lacking NTA-PEG linker. For SAM of higher NTA-PEG content and Au, LeuT seems to be kinetically trapped on the surface probably due to the many contact points between the protein and the highly charged surface as it is typical for polyelectrolytes ². The error bars indicate standard deviations over 3 replicates.

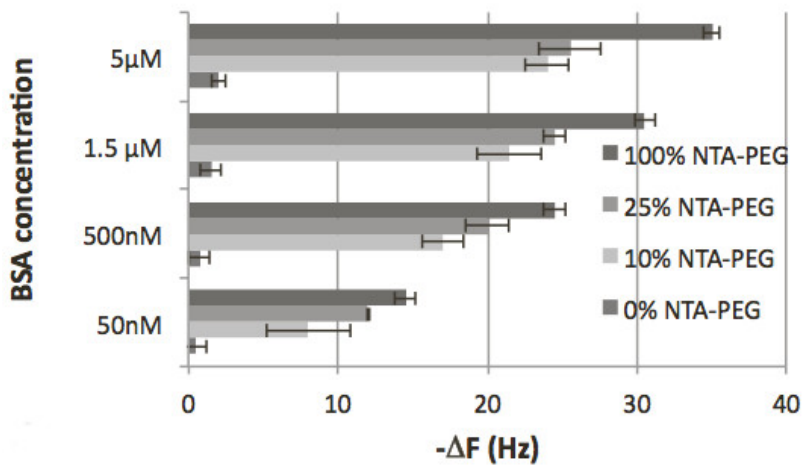


Figure S14. The plotted values correspond to steady state QCM-D signals after BSA addition and extensive rinsing with buffer to eliminate coupling from proteins in the bulk or loosely bound to the surface. The change in frequency decreases (the adsorbed amount increases) progressively with the molar fraction of NTA-PEG linker in the SAM. The error bars indicate standard deviations over duplicates.

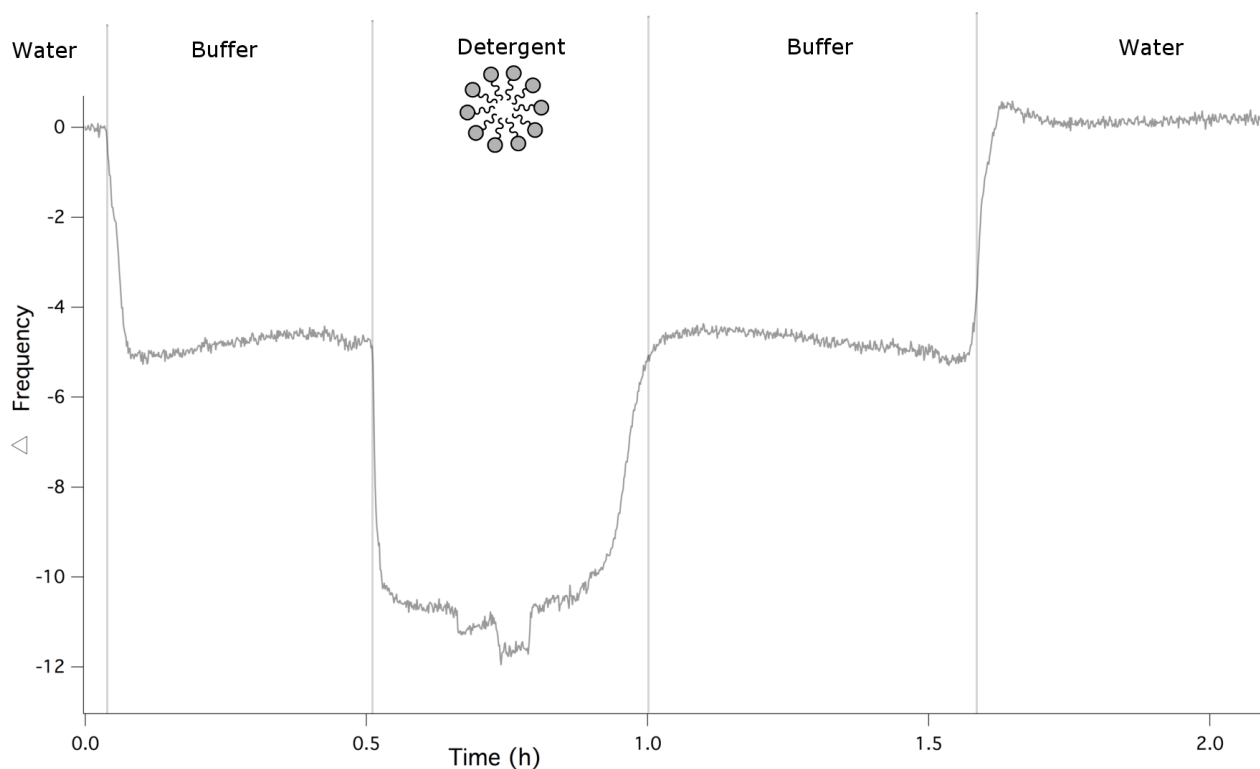


Figure SI5. Reversible binding of the detergent to copper activated 10% NTA-PEG SAM as measured by QCM-D (Change in Frequency, 7th overtone) at 20 °C. The sensor was equilibrated in MilliQ water and it was rinsed with detergent free buffer, DMM containing buffer was added leading to the formation of a detergent monolayer on the surface. Rinsing with detergent free buffer and MilliQ water led to full detergent desorption. Similar traces were observed for MNG-3 containing buffer.

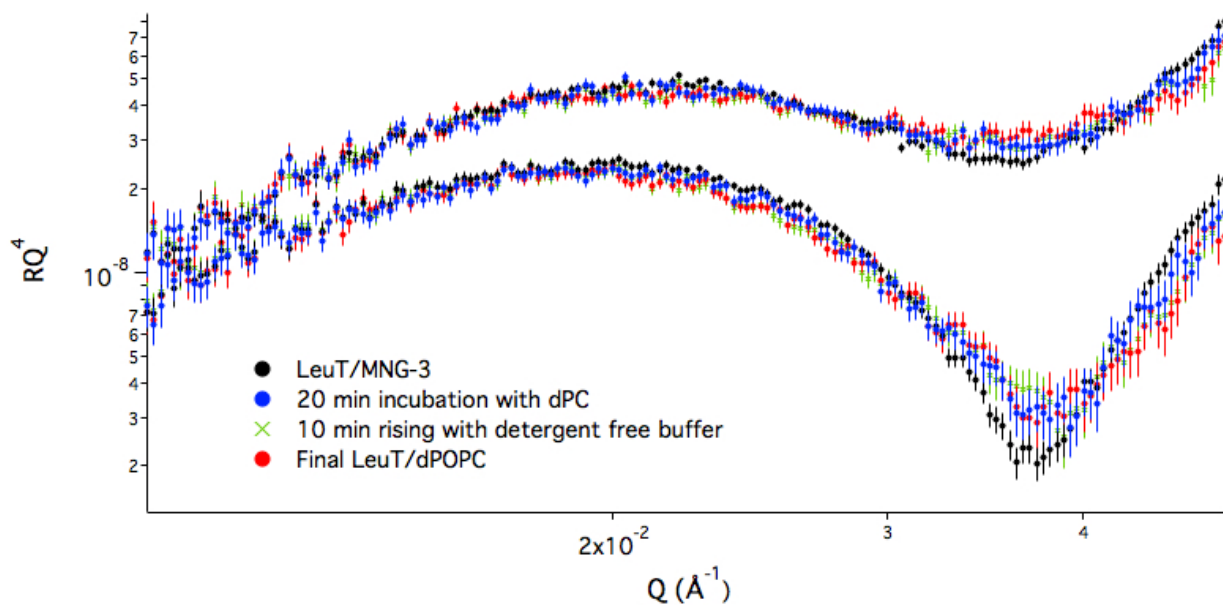


Figure SI6. Magnetic Contrast Polarized Neutron Reflection for adsorbed layers of LeuT in detergent (LeuT/MNG-3), detergent/lipid mixtures (10 min incubation time; LeuT/MNG-3/dPC) or after 10 min and 4h rinsing with detergent free buffer (the final LeuT/dPC). The data show that dPC replaces MNG-3 prior to rinse with surfactant free buffer.

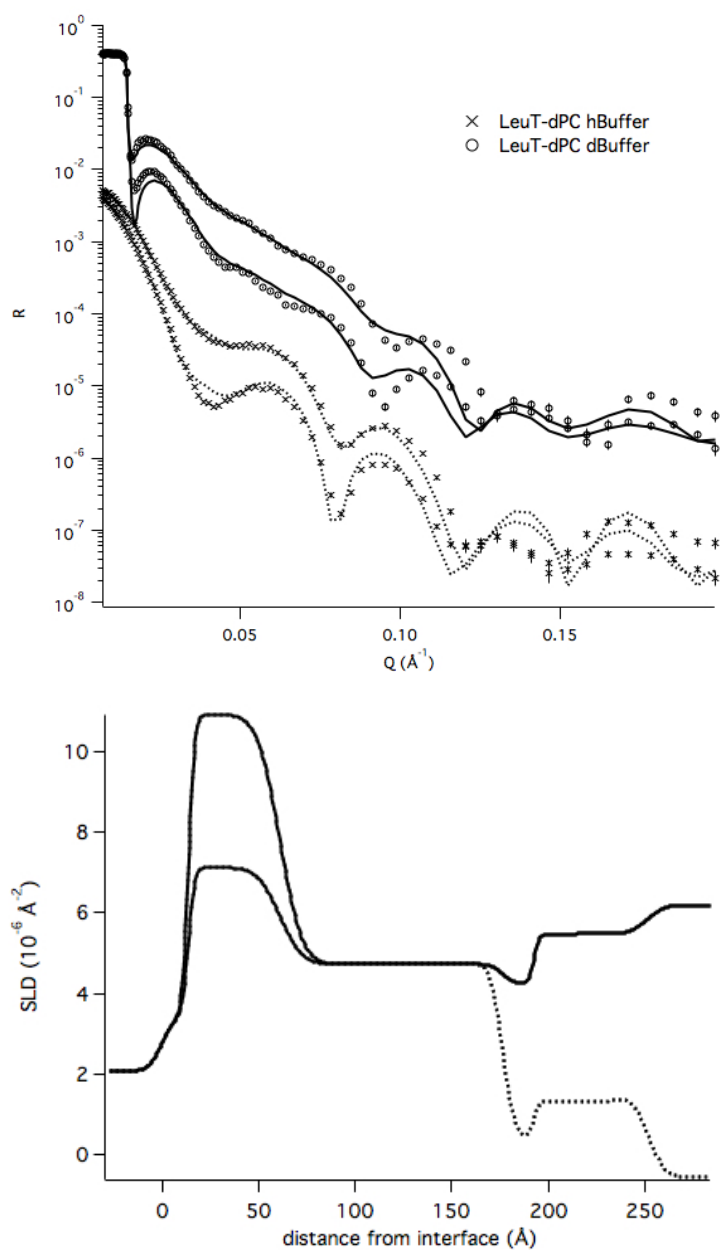
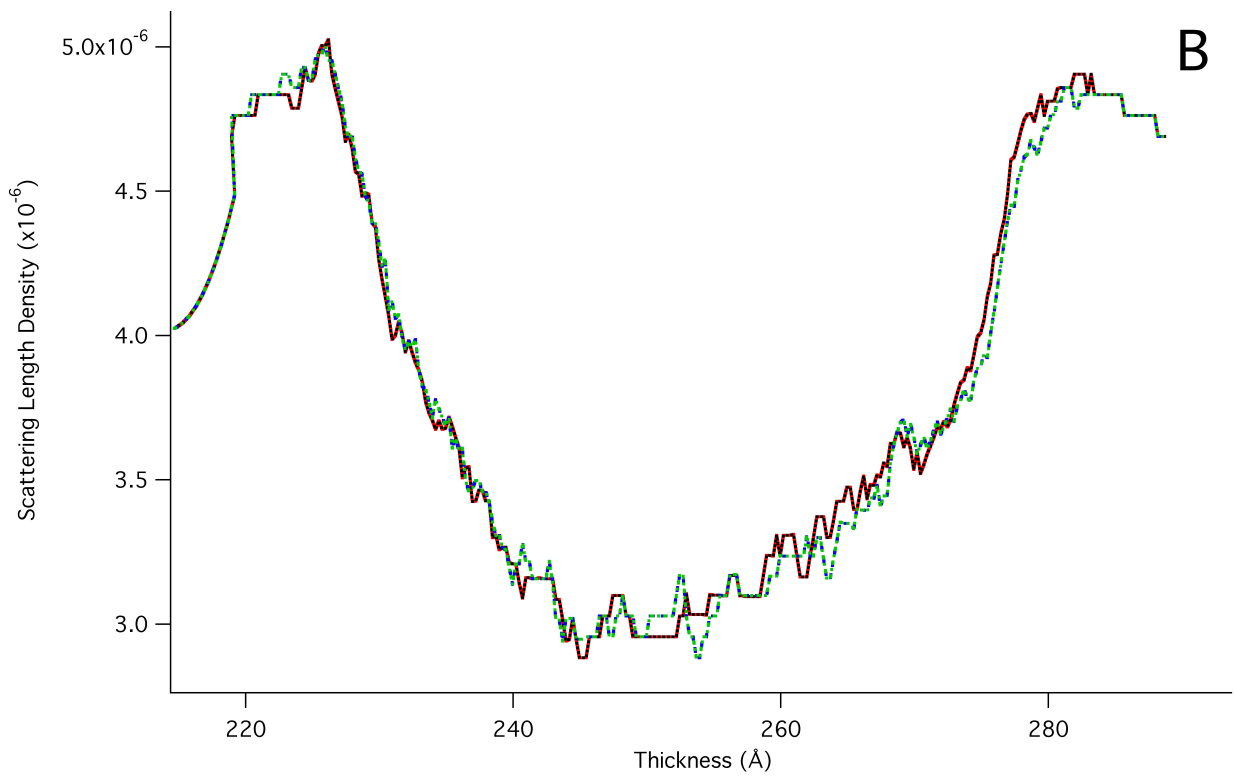
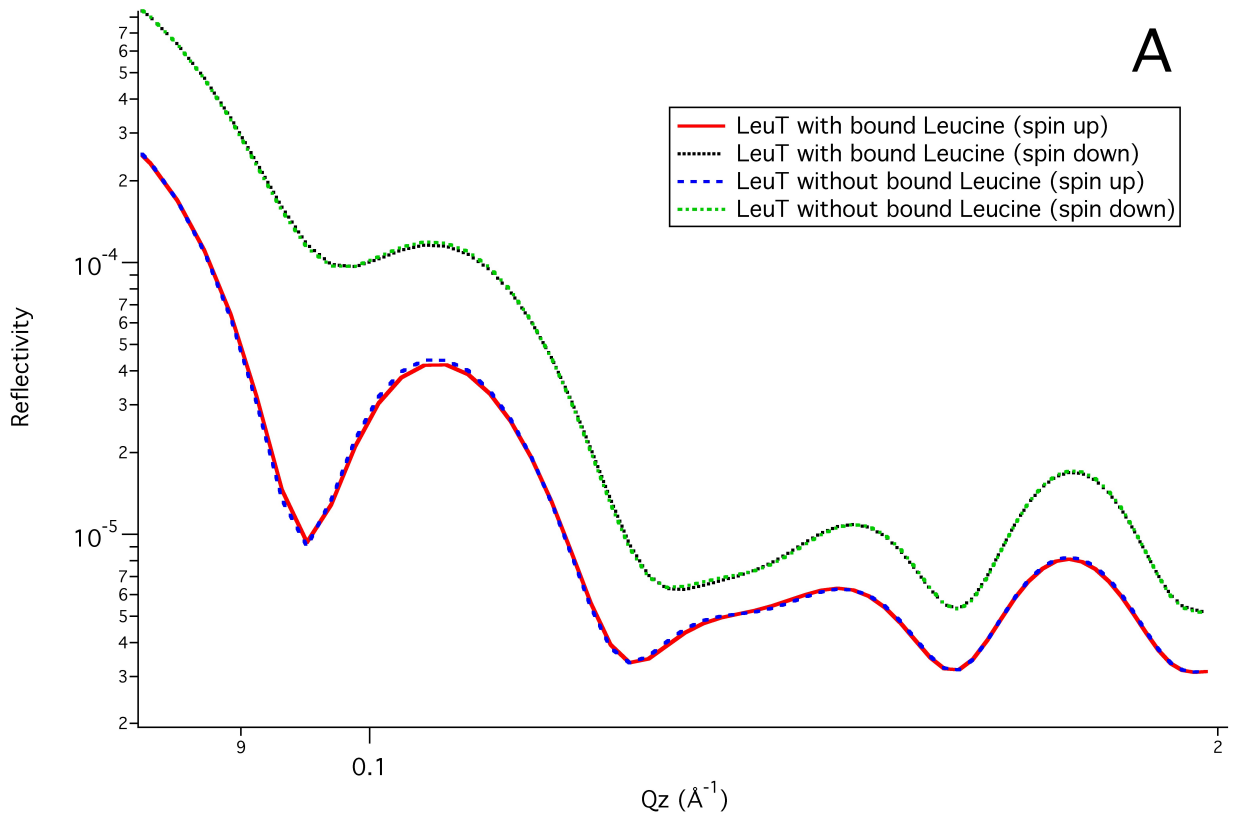


Figure S17. Magnetic Contrast Polarized Neutron Reflection for adsorbed layers of LeuT in dPC (symbols) and best fits using traditional box model approach in which the biomembrane was divided into three layers corresponding to the extracellular, membrane and intracellular parts of the membrane protein. The corresponding scattering length density profile is also included. This demonstrates the advantages of using molecular dynamics simulations to fit Neutron Reflection data of complex films.



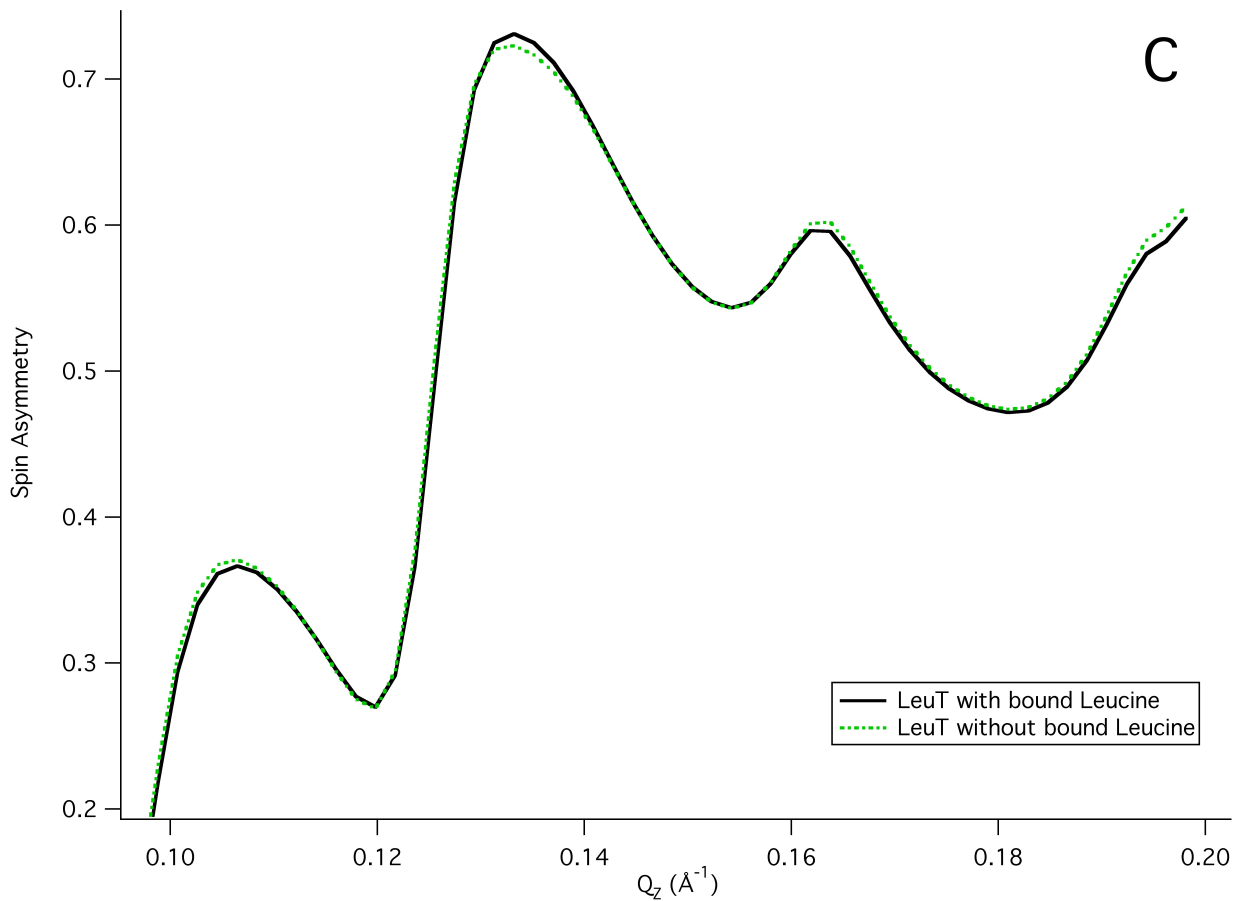


Figure S18. Expanded view of modelled magnetic contrast, polarized neutron reflectivity curves (A) and SLD profiles (B) for LeuT with and without bound leucine as predicted from MD simulations assuming 150 lipids/LeuT and a complete coverage of biomembrane on the surface. The small difference between states that can be seen in the reflectivity curves could be distinguished by plotting the change in spin asymmetry (C). Although this is at the limits of detection using NR, combining this technique with specific deuteration of the LeuT would make the study easier.

Experimental section

Materials.

Palmitoylcholine (POPC) was purchased from Avanti Polar Lipids (Alabaster, AL, USA). Selectively deuterated phosphatidylcholine was purified from a genetically modified *E. coli* strain grown in deuterated medium supplemented with deuterated glycerol and deuterated choline as described earlier.³ Unless stated otherwise, all other chemicals were purchased from Sigma-Aldrich Denmark and used as received without further purification. MilliQ water was used for preparation of aqueous solutions. All solvent ratios are v/v. NMR spectra were recorded on a Bruker Avance 300 spectrometer with a BBO probe. The chemical shifts are referenced to the residual solvent signal. Assignments were aided by H,H COSY and gHSQC experiments. Mass determinations (high resolution MS, HR-MS) were performed on a Micromass LCT instrument with an ESI probe. Analytical HPLC was performed on a Dionex Ultimate 3000 system with Chromeleon 6.80 software; a linear gradient flow of MeCN-H₂O (0.1% formic acid) was used for separations on a C₁₈ column (Gemini-NX, 3 μm, 50x4.6 mm) from Phenomenex. Silica gel 60 (0.015-0.040 mm) from Merck was used for vacuum liquid chromatography (VLC).

Detergent free buffer was made using 50 mM Tris-HCl, 199 mM KCl, 1 mM NaCl set at pH 8. When indicated, this buffer was supplemented with detergent to a concentration of 0.05 w/w% DDM (Anatrace, USA) and 0.005 w/w% MNG-3 (Anatrace, USA). These concentrations correspond to 5 times the surfactant's critical micellar concentration.

Protein expression and purification.

Purification of the wild-type of the leucine transporter (LeuT WT) from *Aquifex aeolicus* was performed similarly to the protocol described previously.⁴ Briefly, LeuT WT was expressed in *E. coli* C41(DE3) strain transformed with pET16b encoding C-terminally 8xHis-tagged transporter kindly provided by Dr E. Gouaux, Vollum Institute, Portland, Oregon, USA. Briefly, isolated bacterial membranes were solubilized in 1 % DDM or MNG-3 followed by Immobilized metal ion affinity chromatography using nickel-charged affinity resin (Life Technologies, Denmark). Subsequently, bound protein was eluted in 20 mM Tris-HCl (pH 8.0), 200 mM KCl, 20 % glycerol, 300 mM imidazole and 0.05 % DDM or in the identical buffer containing 0.005 % MNG-3 instead of DDM. Subsequently, all LeuT samples were dialyzed for approx. 16 h at +4 °C against the respective elution buffer without imidazole.

Synthesis of (S)-4-Carboxy-3-(carboxymethyl)-24-mercapto-10-oxo-13,16,19,22-tetraoxa-3,9-diazatetracosanoic acid (NTA-PEG4-thiol).

15-Tritylmercapto-4,7,10,13-tetraoxapentadecanoic acid monohydrate (54 mg, 0.10 mmol) was dissolved in tetrahydrofuran (0.5 mL). Triethylamine (18 L, 0.12 mmol) was added followed by *O*-(*N*-succinimidyl)-1,1,3,3-tetramethyluronium tetrafluoroborate (36 mg, 0.12 mmol). The resulting suspension was homogenized by addition of *N,N*-dimethylformamide (0.25 mL) and stirred for 16 h at room temperature. Water (3 mL) was added and the resulting precipitate was collected by centrifugation and decantation. The precipitate, *N,N*-bis(carboxymethyl)-*L*-lysine hydrate (39 mg, 0.15 mmol), and potassium carbonate (83 mg, 0.6 mmol) were dissolved in water-MeCN 1:1 (4 mL). The reaction mixture was stirred for 16 h at room temperature and then concentrated. The residue was acidified (HOAc) and purified on a C₁₈ Sep-Pak from Waters (eluting with H₂O-MeCN 4:10:1 containing 1% HOAc) to provide 44 mg of the S-trityl protected product as a clear oil. ¹H NMR (300 MHz, CD₃OD): δ= 7.44-7.37 (m, 6H; Tr), 7.33-7.18 (m, 9H; Tr), 3.69 (t, *J*=6.2 Hz, 2H; N₂COCH₂CH₂O), 3.65-3.52 (m, 14H), 3.49 (dd, *J*=6.5 and 8.0 Hz, 1H; NCH(COOH)CH₂), 3.46-3.41 (m, 2H; CH₂OCH₂CH₂S₂Tr), 3.28 (t, *J*=6.7 Hz, 2H; OCH₂CH₂S₂Tr), 3.18 (bt, *J*=6.2 Hz, 2H; CH₂CH₂NHCO), 2.42 (bt, *J*=6.3 Hz, 2H; N₂COCH₂CH₂O), 2.39 (t, *J*=6.8 Hz, 2H; CH₂S₂Tr), 1.88-1.75 (m, 1H; NCH(COOH)CH), 1.73-1.60 (m, 1H; NCH(COOH)CH'), 1.59-1.40 (m, 4H). HR-MS (ES): calcd for C₄₀H₅₂N₂O₁₁S [M+Na]⁺ 791.3184; found 791.3174. This material was deprotected by stirring with a trifluoroacetic acid-dichloromethane-triethylsilane 1:1:0.1 v/v/v cocktail for 10 min. The solution was concentrated and purified over a plug of silica to provide the desired NTA-PEG4-thiol (37 mg, 57% overall yield) as its trifluoroacetate salt.

HR-MS (ES): calcd for C₂₁H₃₈N₂O₁₁S [M+H]⁺ 527.2269; found 527.2315.

Synthesis of 14-Mercapto-3,6,9,12-tetraoxatetradecanol (PEG4-thiol).

Tetra(ethylene glycol) (194 mg, 1 mmol) was dissolved in dry tetrahydrofuran (12 mL) under argon, followed by addition of PS-PPh₃ (986 mg, 1.5 mmol, 1.52 mmol/g) and triphenylmethanethiol (276 mg, 1 mmol). Under stirring, a solution of diisopropylazodicarboxylate (304 mg, 1.5 mmol) in dry tetrahydrofuran (8 mL) was added drop wise. The mixture was stirred for 4 h and then left unstirred for 16 h at room temperature. The resin was filtered off on a pad of Celite, and the filtrate was concentrated by rotary evaporation. The residue was purified by VLC (diethylether-heptane 1:8→1:0) to provide 129 mg of the mono-S-trityl protected product as a clear oil. ¹H NMR (300 MHz, CD₃Cl): δ= 7.45-7.38 (m, 6H; Tr), 7.31-7.17 (m, 9H; Tr), 3.73-3.55 (m, 10H), 3.48-3.43 (m, 2H),

3.30 (t, $J=6.9$ Hz, 2H; $\text{OCH}_2\text{CH}_2\text{S}^{\text{Tr}}$), 2.44 (t, $J=6.9$ Hz, 2H; $\text{CH}_2\text{S}^{\text{Tr}}$). This material was deprotected by stirring with a trifluoroacetic acid-dichloromethane-triethylsilane 1:1:0.1 v/v/v cocktail for 10 min. The solution was concentrated and purified over a plug of silica to provide the desired PEG4-thiol (60 mg, 28% overall yield) as a colorless oil. HR-MS (ES): calcd for $\text{C}_8\text{H}_{18}\text{O}_4\text{S}$ $[\text{M}+\text{H}]^+$: 211.0999; found: 211.1018.

Formation of self-assembled monolayers (SAM).

Gold coated surfaces (deposited by Thierry Bigault, ILL) were cleaned in dry by ozone treatment for 10 min. Then they were immersed in a 2 wt% Hellmanex solution followed by extensive rinsing with MilliQ water. The surfaces were then placed in a 5:1:1 H_2O , H_2O_2 (30%), NH_4OH (25%) solution at 75 °C for 5 min followed by 15 successive rinses with MilliQ water and ethanol. The surfaces were then stored in ethanol. NTAPEG and PEG thiol solutions were prepared at different molar ratios (0, 10, 25 and 100 mol% PEG) to a total concentration of 150 mM. These solutions were prepared either in PBS buffer pH 7.4, ethanol or equal volume mixtures of ethanol and MilliQ water. The surfaces were then dried and placed into small glass vials containing the thiol solutions with their gold layer facing downwards to avoid dust or particle deposition. The surfaces were allowed to react overnight at room temperature. The surfaces were then subjected to extensive rinsing steps with ethanol and MilliQ water, plus a final 10 min bath sonication in ethanol. The surfaces were then kept in ethanol until use.

X-ray photoelectron spectroscopy (XPS).

Experiments were performed in a Kratos AXIS ULTRA^{DLD} vacuum chamber, fitted with a monochromated $\text{Al}_{\text{K}\alpha}$ X-ray source ($h\nu=1486.6$ eV) operated at a power of 150 W. Pass energies used were 160 eV and 20 eV for wide scans and high resolution scans respectively. The Au $4f_{7/2}$ peak was used for binding energy calibration at 84 eV. Samples were taken out of the solution and rapidly dried out with clean nitrogen flow before introduction to the vacuum chamber.

Methodology Used to Combine MD Simulation Vectors for Analysis of NR Data.

A step-by-step outline of the methods used to combine MD simulation vectors for a protein embedded biomembrane with NR SLD profiles is given below:

1. Extract the z-density vectors from MD simulations for the (a) lipid heads and tails, (b) water distribution through the membrane and (c) protein distribution.
2. Normalize the vectors to the number density for each component individually.

3. Generate a scattering length density (SLD) profile for each vector, based on the calculated scattering cross section for each component.
4. Combine the lipid head, tail and water SLD profiles using the combination:

$$Lipid_Water_{SLD} = LipidHead_{SLD} + LipidTail_{SLD} + (Water_{SLD} * WaterRatio)$$
This ensures a 1:1 lipid head to tail ratio while the *WaterRatio* is kept as a free parameter which can be fitted using the modeling software. This was necessary to improve the fit quality as it was found that the water content per lipid in the membrane patches was greater than that in the idealized MD simulations. Additionally, by taking this approach the distribution of water molecules through the membrane from MD simulations was maintained in the analysis.
5. Combine the $Lipid_Water_{SLD}$ with the protein SLD distribution, normalizing the two by their volume ratio and allowing an additional free parameter *LipidsPerProtein*, which can be used to fit the number of lipids associated with each protein.
6. Scale this composite SLD profile by a *MembraneCoverage* parameter, where:

$$MD_{SLD} = (Lipid_Water_Protein_{SLD} * MembraneCoverage) + (Bulk_{SLD} * (1 - MembraneCoverage)).$$
This was necessary to allow for the incomplete coverage of the LeuT-lipid biomembrane on the surface.
7. Combine the generated MD_{SLD} with the SLD profile fitted for the lower supporting layers (in this case NTA-PEG-Au-Ni/Fe-SiO₂-Si fitted separately). Two additional parameters were necessary at this stage to ensure the correct overlap between the two SLD profiles. These parameters defined the cut-off for each individual SLD profile when contributing to the overall SLD profile.
8. Continue data analysis as usual, allowing the free parameters defined above to be varied within constraints to find the best fit to the NR data.

References

1. Castner, D. G.; Hinds, K.; Grainger, D. W., X-ray Photoelectron Spectroscopy Sulfur 2p Study of Organic Thiol and Disulfide Binding. *Langmuir* **1996**, *12*, 5083-5086.
2. Holmberg, K.; Jönsson, B.; Kronberg, B.; Lindman, B., *Surfactants and Polymers in Aqueous Solution*. Wiley: 2002.
3. (a) Maric, S.; Skar-Gislinge, N.; Midtgaard, S.; Thygesen, M. B.; Schiller, J.; Frielinghaus, H.; Moulin, J. F.; Haertlein, M.; Forsyth, V. T.; Pomorski, T. G.; Arleth, L., Stealth carriers for low-resolution structure determination of membrane proteins in solution. *Acta Crystallographica Section D Biological Crystallography* **2014**, *70*, 317-328; (b) Maric, S.; Thygesen, M. B.; Schiller, J.; Marek, M.; Moulin, M.; Haertlein, M.; Forsyth, V. T.; Bogdanov, M.; Dowhan, W.; Arleth, L.; Pomorski, T. G., Biosynthetic preparation of selectively deuterated phosphatidylcholine in genetically modified *Escherichia coli*. *Applied Microbiology and Biotechnology* **2015**, *99*, 241-254.
4. Chae, P. S.; Rasmussen, S. G. F.; Rana, R. R.; Gotfryd, K.; Chandra, R.; Goren, M. A.; Kruse, A. C.; Nurva, S.; Loland, C. J.; Pierre, Y.; Drew, D.; Popot, J.-L.; Picot, D.; Fox, B. G.; Guan, L.; Gether, U.; Byrne, B.; Kobilka, B.; Gellman, S. H., Maltose-neopentyl glycol (MNG) amphiphiles for solubilization, stabilization and crystallization of membrane proteins. *Nat Meth* **2010**, *7* (12), 1003-1008.